Reprinted from Nature, Vol. 315, No. 6019, pp. 474-477, 6 June 1985

Quaternary structure of the acetylcholine receptor

A. Brisson & P. N. T. Unwin

Service de Physique, Groupe Structures, Département de Recherche Fondamentale, Centre d'Etudes Nucléaires, Grenoble 38041, France
and Department of Cell Biology, Stanford University School of Medicine, Stanford, California 94305, USA

The five membrane-spanning subunits of the acetylcholine receptor have been resolved in electron microscope images and are shown to lie at pentagonally symmetrical positions around the channel over a large fraction of their length. The channel consists of a wide synaptic portion and a narrow portion extending through the membrane into the interior of the cell.

SIGNALLING between excitable cells is commonly mediated by the release of neurotransmitters, which bind subsequently to receptors in the target membranes and induce in them a change of permeability. The nicotinic acetylcholine receptor, the best understood such receptor, effects the change by opening a channel in the membrane through which cations, principally sodium and potassium, diffuse. This action is initiated by the cooperative binding of neurotransmitter to the α-subunits, the two smallest of five (stoichiometry $\alpha_2\beta\gamma\delta$) assembled in a ring around the channel (see refs 1-3 for review).

The complete amino-acid sequences of the four types of polypeptide comprising this receptor have recently been deduced[4-7] and indicate extensive homology between the subunits (see ref. 8 for review). Predictions based on these data suggest a common motif of secondary structure for the portions of the subunits inside the lipid bilayer[9,10], with features having important implications concerning the movement of ions through the channel and the mechanism of the gating event[11,12]. An understanding of the molecular details now requires direct structural information on the different transitional states.

Here we report on a quaternary configuration of the acetylcholine receptor, determined by three-dimensional electron image analysis of tubular crystals grown from native membrane vesicles. Previously, a pentagonal molecular outline had been resolved in individual images of stained tubes, suggesting that the subunits are disposed regularly around the channel[13]. The three-dimensional maps obtained by combining information from many images now reveal details of the subunits and of the channel at different levels throughout the structure. We demonstrate that there is indeed an approximate 5-fold axis of symmetry along the channel axis over a large fraction of the molecule extending from within the lipid bilayer into the synaptic cleft.

Table 1 Three-dimensional data from images of tubes

	Frozen	Stained
No. of images*	35	52
Range of tilt angles	0-60°	0-65°
No. of independent lattice lines†	21	24
No. of Fourier terms used in synthesis‡	208	271
Average phase error/image§	13.5°	11.9°

* Values for the axial ratio b/a and included angle γ were 1.787 ± 0.01, $120.17 \pm 0.19°$ (frozen) and 1.797 ± 0.01, $117.33 \pm 0.48°$ (stained); from 20 measurements, with a, b and γ as defined previously[13]. Thus, the ratio of lateral to longitudinal dimensions is ~5% smaller for the stained than for the frozen tubes.

† Data include all significant lattice lines (except for the (0, 0)) to a resolution of 25 Å; these are the (0, 2), (0, 3), (0, 4), (0, 5), (1, −5), (1, −4), (1, −3), (1, −2), (1, −1), (1, 0), (1, 1), (1, 2), (1, 3), (2, −5), (2, −4), (2, −3), (2, −2), (2, −1), (2, 0), (3, −3), (3, −1) lattice lines in both cases, and in addition the (0, 1), (3, −5), (3, −2) for the tubes in stain.

‡ Obtained by sampling the continuous amplitude and phase curves at regular 0.0025-$Å^{-1}$ intervals.

§ Based on cumulative comparisons of individual peaks over a range of 0.003 $Å^{-1}$ along the lattice lines.

Data collection and analysis

The tubes, which were prepared from the electric organ of the ray *Torpedo marmorata*, are composed of receptors arranged in a p2 surface lattice and oriented with the synaptic side outwards[13]. They are flattened against the support film during preparation (see Fig. 2 legend), forming two almost planar

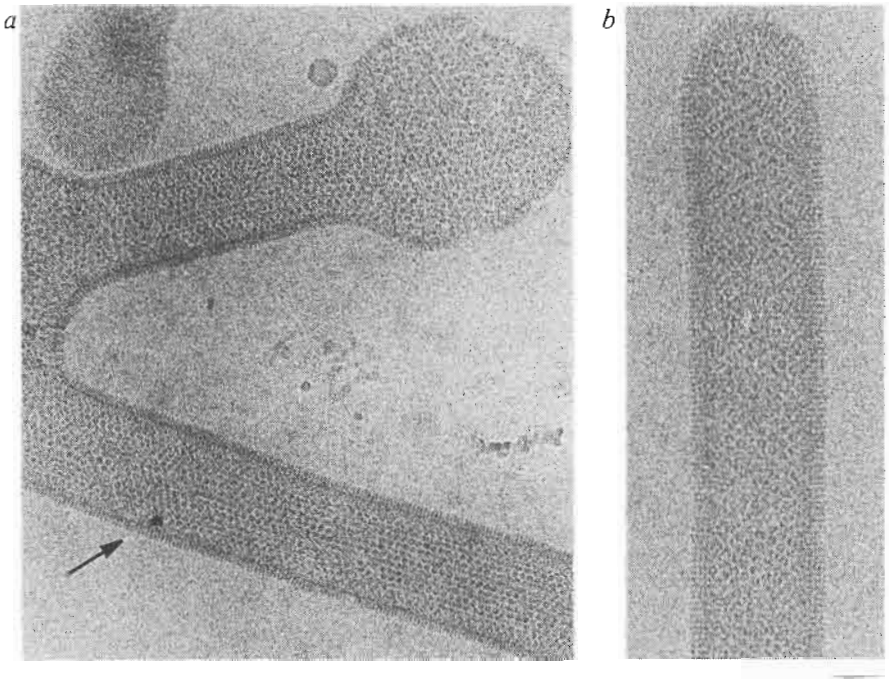

Fig. 1 Electron microscope images of tubular crystals of acetylcholine receptor embedded in thin films of frozen buffer (100 mM Tris-HCl, *p*H 6.8). The complex patterns arise from superposition of *en face* views of the receptors located on the top and bottom surfaces. Striated zones at the tube borders are a result of the receptors being viewed more nearly from the side; when aligned parallel to the tube axis, as in *a*, the receptors in these zones form distinct 120-140-Å wide bands (arrow) and seem to be viewed exactly from the side. Magnifications: *a*, ×112,000; *b*, ×182,400.

superposed layers (Fig. 1). Images of the tubes in frozen solution and in negative stain were obtained to provide information on the complete protein and the hydrophilic surfaces, respectively.

For the analysis, all the selected tubes had surface lattices in orientations close to the example in Fig. 1*b*; therefore, variations in their unit cell parameters were less than described previously[13]. The tubes were tilted at angles of up to 65° to the incident electron beam and the amplitudes and phases of the Fourier components were determined to a resolution of 25 Å from digitized areas of these images. Data were then combined cumulatively by standard methods[14] to map the continuous variations of amplitude and phase along each reciprocal lattice line (Fig. 2). The three-dimensional Fourier syntheses were from the terms obtained by sampling these curves at regular intervals and assuming the unit cell dimensions in the plane of the membrane to be $a = 90.0$ Å, $b = 160.8$ Å, $\gamma = 120.2°$, determined from the frozen specimens. The densities synthesized from the stained specimens were multiplied by -1 to correct for their opposite contrast. Further details are given in Table 1.

The similarity between the two three-dimensional maps was evaluated by comparing sections at various levels throughout the two structures. The sections were parallel to the plane of the membrane and the comparisons included all the densities in a single unit cell. The best overall correlation was achieved with a relative displacement of 11 Å perpendicular to the membrane between the origins of the two maps, reflecting differences between the centres of scattering density for the two cases. Corresponding values for the correlation coefficients were >0.8 over most of the ~140 Å length in which features were clearly contrasted (Fig. 3), except for a narrow zone identified as the hydrophobic core of the bilayer (see below). Hence, with the exception of this zone, the two maps resemble each other closely. Exact correspondence, particularly at the extremities of the structure, is not expected because of minor alterations resulting from, for example, drying of the stain[15].

Structure of the receptor

The three-dimensional map calculated from the frozen tubes (Fig. 4) shows details of the entire receptor molecule, both in the lipid bilayer and in the aqueous surroundings on either side. The molecule is resolved into five rod-shaped subunits (Fig. 4*a*) of about equal cross-section, which lie predominantly perpendicular to the membrane plane. The five subunits are contained within a ~140-Å-long by ~80-Å-diameter cylindrical shell, and delineate a water-filled opening, presumed to be the channel, along the axis of this cylinder.

This map does not distinguish between the portion of the oligomer embedded in the bilayer and those protruding outside, because lipid and water contribute about equally to the image contrast at low resolution. The portions, however, can be identified by correlation with the map from the stained tubes. A ~30-Å zone in that map appears almost featureless—neither the channel nor the surrounding protein is visible—and must correspond to the hydrophobic core of the bilayer, which is inaccessible to the stain. Consequently, there is a length of ~30 Å, the correlation coefficients of which have particularly low values (Fig. 3), and the matching of structural detail is poor (Fig. 5*b*) compared with that on either side (Fig. 5*a*, *c*). Thus the correlation places the hydrophobic core nearest to the cytoplasmic end of the structure, leaving a length of 35–45 Å protruding on this side, compared with ~70 Å on the other.

The channel is nearly 30 Å wide at the synaptic end of the oligomer (Fig. 4*b*, uppermost), but becomes too narrow at the cytoplasmic end to be seen. The way in which the channel

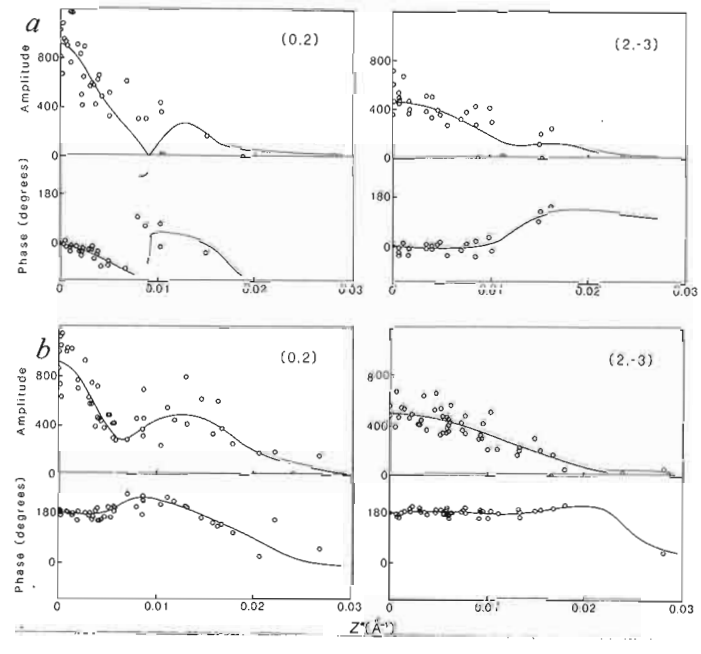

Fig. 2 Comparison of amplitude and phase variations along typical lattice lines after combining images from tubes in: *a*, ice; *b*, stain, according to the 2-sided plane group p21. The continuous curves through the data points were computed by a least-squares method with amplitudes weighted according to the reliability of the corresponding phases[22]. Z^* is the distance from the midpoint of the lattice line.

Methods. Tubes were prepared as described previously[13] and applied to carbon support grids rendered highly charged by glow discharge in amylamine vapour[23]. For freezing, grids were blotted with filter paper for 4 s, then plunged rapidly into liquid ethane cooled to below −130 °C; for staining, they were washed in 2% sodium phosphotungstate *p*H 7.2 and then dried. Frozen specimens were stored under liquid nitrogen and later examined in a Philips EM400 electron microscope using a cold holder maintained at −174 °C. The electron optical magnifications were ×40,800 (ice) and ×28,500 (stain), and images were recorded at 100 kV on Kodak SO163 film developed for 8 min in concentrated D19 developer. A Philips low-dose kit was used to minimize radiation damage and to ensure that all images incorporated in the three-dimensional datasets were of tubes which had received total doses of no more than ~15 electrons per Å^2. Optical adjustments were performed at a nominal magnification on the screen of ×90,000 to minimize variability in focus level from one image to the next. Tube images were evaluated by optical diffraction (see ref. 13) for the extent of structural preservation and degree of flattening, and then evaluated further by computer. For the computer analysis, densitometry and Fourier transformation of the central portion of the tubes were as described previously[13]; criteria for selection of images for incorporation into the three-dimensional datasets included the strength of the diffraction maxima above background and the accuracy with which they fit a regular two-dimensional net. Also, areas of interest were considered unsuitable if the corresponding under-focus values (see below) were outside the range 8–16,000 Å. Variability in lattice parameters between tubes necessitated the use of special methods to derive accurate values of tilt angle and axis. All images were recorded in pairs. With the frozen specimens (*a*) the second image of each pair was of the carbon support film only, after intensifying the electron beam to sublimate the ice. Diffraction patterns from these images displayed a series of concentric rings[24] extending to spacings <10 Å. Defocus values could be measured locally with an accuracy of ±250 Å over a wide range, based on matching such patterns against a calibrated set. Tilt parameters were computed from the defocus values measured at the four corners of each film. Typical errors, estimated by comparing values from the four alternative planes passing through the different sets of three points, were 2° in tilt angle and 4° in direct of tilt axis, slightly larger errors applying to smaller tilts (<10°). With the stained specimens (*b*), the second image was recorded (with negligible in-between irradiation) at another angle of tilt, differing from the first by a pre-selected amount (typically 15°). Tilt parameters were computed from the changes in reciprocal lattice geometry between the two images. In this case the independent values obtained from the two sides of each tube could be compared, and the errors indicated were found to be of similar magnitude as in the first method.

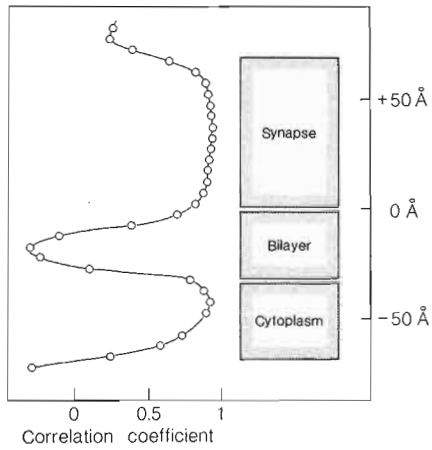

Fig. 3 Plot of correlation coefficients obtained by comparing sections from the three-dimensional maps of the frozen and stained tubes. The ordinate indicates the various levels through the structure, perpendicular to the membrane, at which the values were calculated. The hydrophobic core of the bilayer is identified by a zone showing poor correlation. The synaptic and cytoplasmic domains show good correlation over most of their extent; the poorer correlation near the extremities of the structure may be due to slight flattening of the stained receptors in the direction normal to the membrane plane.

narrows cannot be discerned accurately at the resolution achieved in the present study, but the abrupt exclusion of the anionic stain at the level of the bilayer surface, on the synaptic side, suggests that a large reduction in its diameter occurs in this region.

The cross-sectional area of the membrane-spanning portion of the subunits is of interest because of the different models that have been proposed for the internal structure of this portion. To estimate this value, we assumed the molecular boundary to be at the contour level for which the total enclosed volume of glycosylated protein is 350,400 Å^3, calculated from the composition[8]. The corresponding cross-sectional area per subunit was 540 Å^2, averaged over the extent of the bilayer, whereas for the synaptic and cytoplasmic portions it was 550 and 375 Å^2, respectively. As an approximate check on the value for the cross-section in the bilayer, a three-dimensional map was also calculated with approximate terms included for the central (0, 0) lattice line. These terms were derived from transforms of the striated border regions of tubes, as in Fig. 1*a*, using the (1, 2) lattice line (associated with the striation periodicity) to set the scale for the amplitudes and the origin of the phases. From the molecular boundary now on an absolute scale, a mean value of 500 Å^2 was obtained for the subunit cross-section in the bilayer, in reasonable agreement with the estimate based on protein composition.

Pentagonal symmetry

The five subunits are arranged regularly around the central axis of the receptor for much of its length, so that the structure has approximate pentagonal symmetry about this axis. The r.m.s. departures from exact symmetry are, respectively, 1.2 and 1.4 Å in radius and azimuth averaged over the portion of the protein in the hydrophobic core of the bilayer, and 0.8 and 1.9 Å averaged over the contiguous ~30-Å portion on the synaptic side. The total extent of this symmetrical region comprises about half of the length of the molecule, sufficient to dominate its appearance in projection (Fig. 5*d*). Nearer to the extremities, particularly on the cytoplasmic side, the pentagonal symmetry is not as marked, suggesting more profound structural differences between individual subunits in these regions? On the cytoplasmic side the distribution of mass about the axis of the oligomer is asymmetrical (Fig. 5*c*) and the cross-section is smaller, as if the parts of the subunits here have different lengths.

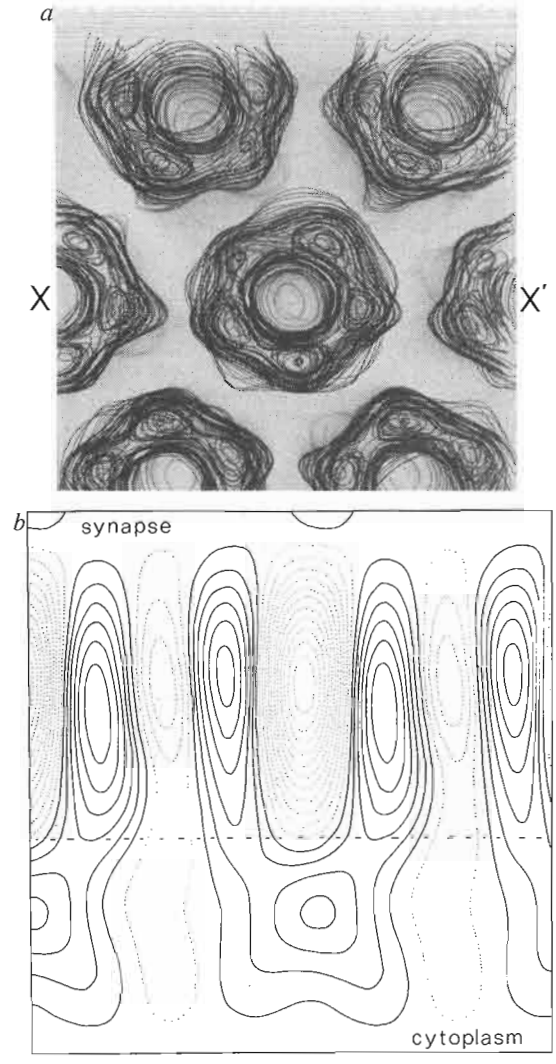

Fig. 4 *a*, Three-dimensional map of receptor molecules in the crystal lattice as they would appear viewed from the synaptic cleft; successive sheets are of sections parallel to the membrane plane separated by spaces corresponding to 5 Å. The centre-to-centre separation between receptors in the horizontal direction corresponds to 90 Å. *b*, Section along the line XX′ in *a*, through the channel axes and perpendicular to the plane of the sheets; the central plane of the bilayer is indicated by the broken line. The phosphotungstate stain is excluded from the channel at a level ~15 Å above this line. Only contours corresponding to regions in which protein is concentrated are shown in *a*; all contours are shown in *b*. The outermost, full-line contours in *a* and *b* are close to the zero contour in Fig. 5 and represent the molecular boundary consistent with the volume calculated from protein composition.

Discussion

The tubular crystals have led to a quantitative description of the quaternary structure of the acetylcholine receptor in a natural lipid-containing environment. The receptor is a cylindrical molecule having almost constant lateral dimensions (mean diameter ~65 Å) except for the part on the cytoplasmic side of the bilayer, which is narrower. It is composed of five rod-shaped subunits, each up to ~140 Å long. They lie approximately perpendicular to the membrane plane and are asymmetrically placed in relation to the bilayer, having two to three times more of their combined mass on the synaptic than on the cytoplasmic side. Subunits are similar in cross-section and are arranged symmetrically around a central opening, the presumed channel through which cations diffuse. The channel is partitioned equally into a wide (25–30-Å diameter) portion at the synaptic end of the structure and an unresolved narrow portion extending through the membrane into the interior of the cell.

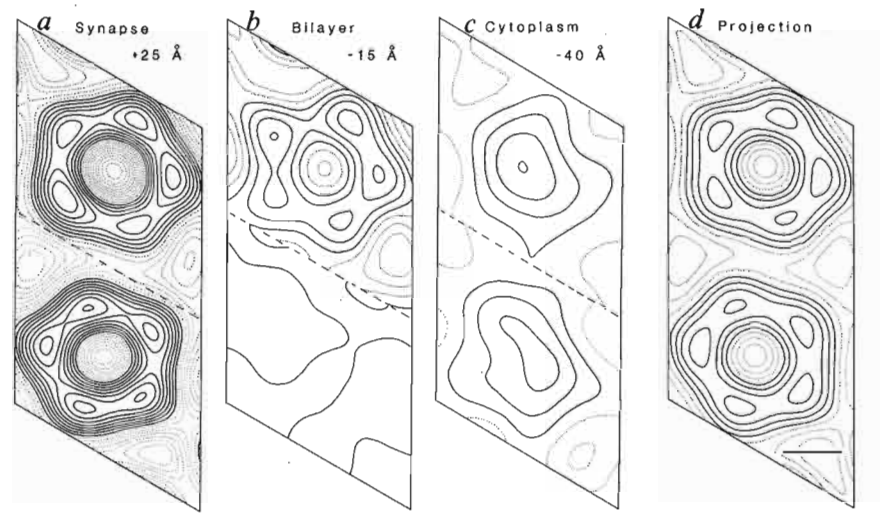

Fig. 5 *a–c*, Sections at different levels through a unit cell from the three-dimensional maps; *d*, the projected structure in frozen solution. The pair of receptors shown is thought to correspond to the δ–δ subunit linked physiological dimer[13]. In *a–c* the regions and levels indicated relate to Fig. 3; contours in the upper and lower halves refer to the frozen and the stained tubes, respectively; the two halves are related by symmetry as in *d*. The positive and zero contours are indicated by continuous lines, the negative contours by dotted lines; data from the (0, 0) lattice line, not included in the Fourier syntheses, have only a minor effect on the position of the zero contour. The scale bar (bottom right) corresponds to 25 Å.

In previous studies, electron images of stained molecules, viewed *en face* and from the side, have been used to deduce the overall shape of the protein and channel[16,17,25–27]. Morphological observations have also been combined with X-ray or neutron diffraction data to obtain models for the cylindrically averaged distribution of mass[18,19]. Seen most directly in frozen solution, the molecule appears more elongated and more angular in shape than has generally been supposed.

Identification of the membrane-spanning portion of the structure (Fig. 3) partitions the protein mass on either side in a way that is consistent with models inferred from the amino-acid sequences. However, the probable correctness of different models cannot be evaluated on this basis because of the possibility that the extrinsic cytoplasmic protein of apparent molecular mass 43,000 (ref. 20), thought to be present in the tubes, is bound regularly to the crystallized receptor and contributes some extraneous mass.

A striking aspect of the entire oligomer, previously suspected[1] but not seen until the present study, is that the subunits are arranged in almost equivalent positions around the channel, conferring on the structure an apparent high degree of pentagonal symmetry. This is most exact in the lipid bilayer and over a contiguous ~30 Å region on the synaptic side, and may be even more extensive than observed because minor errors in our data would make it less pronounced. Such symmetry, combined with the observed amino-acid sequence homology, makes it probable that the individual subunits share common features of tertiary organization over the lengths that they are in contact. These properties could be important in facilitating a coordinated movement of all subunits around the channel, such as may occur in switching between different transitional states[8].

The resolution of the analysis described here is insufficient to elucidate the internal structure of the subunits, but the observed details are consistent with models speculating that their membrane-spanning portions are composed of equal numbers of closely packed α-helical rods, or other configurations of the polypeptide chain[28]. The value suggested for the subunit cross-section in this region, 500–540 Å^2, favours models with five α-helices extending through the membrane[10,12] (assuming, for example, a packing similar to that in bacteriorhodopsin[21]).

We thank Dr P. Swann, Gatan Inc., for making available an electron microscope cold holder, and Dr C. Cazaux and his colleagues at the Institut de Biologie Marine, Arcachon for supplying *T. marmorata*. The research was supported by EMBO and Phillipe Foundation Fellowships to A.B. and by a grant from the NIH.

Received 17 January; accepted 19 April 1985.

1. Changeux, J.-P. *Harvey Lect.* **75,** 85–254 (1980).
2. Karlin, A. in *The Cell Surface and Neuronal Function* (eds Cotman, C. W., Poste, G. & Nicolson, G. L.) 191–260 (North-Holland, Amsterdam, 1980).
3. Conti-Tronconi, B. M. & Raftery, M. A. *A. Rev. Biochem.* **51,** 491–530 (1982).
4. Noda, M. *et al. Nature* **299,** 793–797 (1982).
5. Noda, N. *et al. Nature* **301,** 251–255 (1983).
6. Claudio, T., Ballivet, M., Patrick, J. & Heinemann, S. *Proc. nat. Acad. Sci. U.S.A.* **80,** 1111–1115 (1983).
7. Devillers-Thiery, A., Giraudat, J., Bentaboulet, M. & Changeux, J.-P. *Proc. nat. Acad. Sci. U.S.A.* **80,** 2067–2071 (1983).
8. Popot, J.-L. & Changeux, J.-P. *Physiol. Rev.* **64,** 1162–1239 (1984).
9. Noda, *et al. Nature* **302,** 528–532 (1983).
10. Finer-Moore, J. & Stroud, R. M. *Proc. natn. Acad. Sci. U.S.A.* **81,** 155–159 (1984).
11. Lewis, C. A. & Stevens, C. F. *Proc. natn. Acad. Sci. U.S.A.* **80,** 6110–6113 (1983).
12. Guy, H. R. *Biophys. J.* **45,** 249–261 (1984).
13. Brisson, A. & Unwin, P. N. T. *J. Cell Biol.* **99,** 1202–1211 (1984).
14. Amos, L. A., Henderson, R. & Unwin, P. N. T. *Prog. Biophys. molec. Biol.* **39,** 183–231 (1982).
15. Finch, J. T. & Klug, A. *J. molec. Biol.* **13,** 1–12 (1965).
16. Cartaud, J., Benedetti, E. L., Sobel, A. & Changeux, J.-P. *J. Cell Sci.* **29,** 313–337 (1978).
17. Sealock, R. *J. Cell Biol.* **92,** 514–522 (1982).
18. Klymkowsky, M. W. & Stroud, R. M. *J. molec. Biol.* **128,** 319–334 (1979).
19. Wise, D., Karlin, A. & Schoenborn, B. P. *Biophys. J.* **28,** 473–496 (1979).
20. Froehner, S. C. *et al. Proc. nat. Acad. Sci. U.S.A.* **78,** 5230–5234 (1981).
21. Henderson, R. & Unwin, P. N. T. *Nature* **257,** 28–32 (1975).
22. Agard, D. A. *J. molec. Biol.* **167,** 849–852 (1983).
23. Dubochet, J., Lepault, J., Freeman, R., Berriman, J. A. & Homo, J.-C. *J. Microsc.* **128,** 219–237 (1982).
24. Thon, F. *Z. Naturforsch.* **219,** 476–478 (1966).
25. Kistler, J. K. & Stroud, R. M. *Proc. natn. Acad. Sci. U.S.A.* **78,** 3678–3689 (1981).
26. Zingsheim, H. P., Neugebauer, D.-C., Barrantes, F. J. & Frank, J. *Proc. natn. Acad. Sci. U.S.A.* **77,** 952–956 (1980).
27. Bon, F. *et al. J. molec. Biol.* **176,** 205–237 (1984).
28. Criado, M., Hochschwender, S., Sarin, V., Fox, J. L. & Lindstrom, J. *Proc. natn. Acad. Sci. U.S.A.* **82,** 2004–2008 (1985).